Thin Solid Films 651 (2018) 13–17

Contents lists available at ScienceDirect

Thin Solid Films

journal homepage: www.elsevier.com/locate/tsf

Density functional theory based interfacial studies of $ABO_3/SrTiO_3$ (A = La, Y, Sc, B = Al, Ga) and its relation to polar catastrophe

Jinhyung Cho[a,*], Hyoungjeen Jeen[b], Eunsoo Cho[c]

[a] RCDAMP and Department of Physics Education, Pusan National University, Busan 46241, Republic of Korea
[b] Department of Physics, Pusan National University, Busan 46241, Republic of Korea
[c] Department of Materials Science and Engineering, Seoul National University, Seoul 08826, Republic of Korea

ARTICLE INFO

Keywords:
DFT
$LaAlO_3/SrTiO_3$ thin films
Interfaces
Density of states
Ferroelectrics

ABSTRACT

We have studied the density functional theory of epitaxially strained ABO_3 (A = La, Y, Sc, B = Al, Ga) films on $SrTiO_3$ (001) crystals with SrO- and TiO-terminations to investigate polar catastrophe induced by the epitaxial thin film growth. Interfacial polar nature of the strained films depends on the type of cations. While lanthanum based perovskite films produces polarity based on the ionic nature of interfacial atoms, the smaller cations show rather opposite polarities arising from progressive ferroelectric structural distortion acting opposite to the polar nature of cation ions.

1. Introduction

Heterogeneous interfaces of $SrTiO_3$ crystals have long been studied due to their very versatile properties arising from presence of interfaces lacking in bulk materials as well as termination-dependent conducting properties. While a few layer of $LaAlO_3$ overgrowth on TiO-terminated surface of $SrTiO_3$ exhibits two-dimensional conducting interface, the insulating behavior of $LaAlO_3$ interface has been observed on the overgrowth on SrO-terminated surface [1]. Originally, this spur many theoretical and experimental studies to investigate the interface properties, indicating that the origin of the properties result from the polar catastrophe from the electric field by the net charge of LaO overlayer on TiO-terminated surface [2–4]. In addition, there have been many additional experimental and theoretical works by changing cations and anions showing the metallic nature of interfaces from various thin film growth on $SrTiO_3$ such as $LaGaO_3$ [5,6]. These kinds of experiments support for the polar catastrophe as the origin of the conducting properties. On the other hand, the mechanism of the intriguing properties was proposed to be extrinsic by the intermixing of the cations due to film growth mechanism of the pulsed laser deposition and involvement of energetic particles during the film growth [7–9].

To further clarify the origin of the conducting interfaces unambiguously, it is necessary to study as many perovskite compounds as possible experimentally and theoretically. In this paper, we will report density functional theory calculations of $ABO_3/SrTiO_3$ with epitaxially strained ABO_3 perovskite structures on both TiO- and SrO-terminated surfaces of $SrTiO_3$ (001). Epitaxially grown strained films have shown interesting physics that was not observed in bulk materials. Typical heteroepitaxial growth of films on substrates with different lattice constants, as shown in this manuscript for the case of ABO_3 on $SrTiO_3$ (001), undergoes several steps during the film growth. First step of the film growth would be epitaxially grown strained ultrathin films matching with the in-plane lattice constant of substrate $SrTiO_3$. This type of epitaxial growth would persist up to critical thickness of the grown ABO_3 epitaxial films. The next step of the film growth would be island-like relaxed ABO_3 growth with misfits to relax the strains. In this manuscript, we have theoretically studied epitaxially grown strained films. To simplify the theoretical studies, we assume that the ABO_3 (A = La, Y, Sc, B = Al, Ga) layers were grown epitaxially on cubic (001) $SrTiO_3$ surfaces with tetragonal structures to accommodate the structural distortion and strain on both terminations. Therefore, there exist both tensile and compressive strains depending on size of cation atoms in the perovskite structures, so that the assumed epitaxially grown tetragonal perovskite structure of ABO_3 grown on $SrTiO_3$ may not be ideal ground state structures. To be specific, $LaAlO_3$ forms trigonal R-3c structure with pseudo-cubic lattice spacing of 3.828 Å, $YAlO_3$ forms orthorhombic Pnma perovskite structure with lattice constants of 5.125, 5.249, and 7.291 Å with pseudo-cubic lattice spacing of 3.668 Å, perovskite $ScAlO_3$ forms at high pressure with orthorhombic Pnma perovskite structure with 4.964, 5.252, and 7.261 Å with pseudo-cubic lattice spacing of 3.613 Å, $LaGaO_3$ forms orthorhombic Pnma perovskite structure with 5.499, 5.511, and 7.764 Å with pseudo-cubic lattice spacing of 3.893 Å, $YGaO_3$ forms $P6_3cm$ hexagonal structure with 6.065, 6.065, and 11.615 Å, and $ScGaO_3$ with Pnma structure with

* Corresponding author.
E-mail address: jinhcho@pusan.ac.kr (J. Cho).

https://doi.org/10.1016/j.tsf.2018.02.001
Received 19 October 2017; Received in revised form 28 January 2018; Accepted 2 February 2018
Available online 04 February 2018

5.125, 5.249, and 7.291 Å [10]. To justify our theoretical works, it is assumed that the growth of the metastable tetragonal perovskite structures on (100) $SrTiO_3$ is possible if the ABO_3 films are thin enough below the critical thicknesses.

2. Theory

The calculations were performed with Quantum Espresso packages [11] based on PWScf with pbesol of revised Perdew-Bruke-Ernzerhof (PBE) generalized gradient approximation that better predicts the lattice spacing for the solids [12]. The used pseudopotentials were based on ultrasoft type pseudopotentials obtained from GBRV data bases. The cutoff energy of plane wave base Kohn-Sham wavefunctions was 36.75, and 360 Ry was used for the charge density energy cutoff. For the Ti atoms, we used Hubbard U of 5 eV. In addition, we also calculated the average potential with respect to pristine vacuum theoretically. To calculate the surface and interface properties, the symmetric geometries of slab with central 6 layers of pseudo-cubic $SrTiO_3$ (STO) in the center and 6 layers of ABO_3 on both sides with total 93 atoms were used. Initially, the vacuum distance of ~24 Å between slabs was used to eliminate the spurious surface dipole electric field. The central atomic positions of SrO, TiO_2, and SrO layers were fixed to simulate the bulk lattice of $SrTiO_3$. As a result, the in-plane lattice constants of the films were fixed to the experimental value of 3.906 Å. All of the calculations presented here were performed with 2 × 2 × 1 Monkhorst Pack k-point mesh. We double checked the results with 5 × 5 × 5 Monkhorst Pack k-point mesh, showing the same behaviors. During the structural relaxations of $ABO_3/SrTiO_3$, all atoms were relaxed until the forces were smaller than ~0.0026 eV/Å. The final distances between slabs changed after the structural relaxations depending on cations. However, the vacuum distances between two slabs were still large enough to minimize the electrostatic effect.

3. Results and discussion

Fig. 1 shows schematic structures of $ABO_3/SrTiO_3$ (001) for the density functional theory calculations studied in this paper. The structures consist of 6 cubic units of $SrTiO_3$, where the central TiO_2 and 2 layers of SrO next to it were fixed to simulate the bulk crystal of $SrTiO_3$. We added 6 units of ABO_3 on both sides of $SrTiO_3$ interfaces to reduce the dipole field induced by asymmetric surfaces if we calculate asymmetric structures instead. The interface atoms indicated by the arrows are A for TiO-termination and Sr for SrO-termination, respectively. Experimentally, it is observed that the 6 layers of ABO_3 produce two-dimensional conductivity at the interface in $LaAlO_3$ systems [13], so that we fixed 6 layers of ABO_3 in this paper to see the change of densities of states with cations.

Fig. 2(a) shows projected densities of states of atomic species after the structural relaxations of $LaAlO_3/SrTiO_3$, $YAlO_3/SrTiO_3$ and $ScAlO_3/SrTiO_3$ and Fig. 2(b) shows projected densities of states of atomic species after the structural relaxations of $LaGaO_3/SrTiO_3$, $YGaO_3/SrTiO_3$ and $ScGaO_3/SrTiO_3$. The Positive data represent the densities of states of ABO_3 of TiO-terminated $SrTiO_3$, while the negative data represent the densities of states of ABO_3 on SrO-terminated $SrTiO_3$. The data were obtained after relaxing the atomic positions with respective $ABO_3/SrTiO_3$ structures. The data indicate that the density of states of $LaAlO_3/SrTiO_3$ shows the conducting or insulating behavior depending on the termination, as seen by the closing of the band gap in the TiO-terminated $SrTiO_3$, while SrO-terminated $SrTiO_3$ still remains the gapped states. The vertical dotted lines in the figures show the fermi energy of TiO-termination. This is consistent with many previous studies [2,3]. On the contrary, the densities of states of $YAlO_3/SrTiO_3$ show both insulating characteristics independent of terminations as shown by the gapped states on both terminations. Finally, the densities of states of $ScAlO_3/SrTiO_3$ show conducting behavior with finite densities of states at the fermi level on both terminations. This marks the difference with larger cation of La. In addition, as shown in the Fig. 2(b), the generic behavior of Ga-based perovskites with respect to cations La, Y and Sc is similar to those of Al, indicating the similar origin for this behavior. The bandgaps of the ABO_3 films were obtained by plotting all partial densities of states of given ABO_3 films relative to the fermi energy levels. The bandgaps of TiO-terminated $LaAlO_3$, $YAlO_3$, $ScAlO_3$, $LaGaO_3$, $YGaO_3$ and $ScGaO_3$ are 0.00, 1.72, 0.00, 0.97, 1.52 and 0.00 eV, respectively. The bandgaps of SrO-terminated $LaAlO_3$, $YAlO_3$, $ScAlO_3$, $LaGaO_3$, $YGaO_3$ and $ScGaO_3$ are 2.22, 2.69, 0.00, 2.33, 1.75 and 0.00 eV, respectively. Since we can expect the change of work functions with respect to the two terminations by different polar nature, we calculated microscopic potentials along (001) averaged in the planes parallel to the surfaces. The calculated data show oscillation along (001). By averaging the microscopic potential by the structural periodicity along the z axis roughly of 3.906 Å, we can get average potential values. However there still exist small oscillations due to different periodicity of lattice constants of ABO_3. Therefore, we further averaged the average potentials to obtain macroscopic average values. Fig. 3 shows the macroscopic average potential along (001) of both terminated $ABO_3/SrTiO_3$. Compared to the data of the projected densities of states shown in Fig. 2(a) and (b), it seems that the conducting and insulating behaviors of the films are directly related to the slope of macroscopic potentials in ABO_3 originating from the internal electric field induced by the interface charges and structural distortion. Unlike the simple ionic picture of interfacial ionic La cation, the internal electric fields systematically change from positive to negative toward the surface as the ionic size becomes smaller. In the case of Y cation, the internal field is relatively flat on both terminations, resulting in the gapped states seen in Fig. 2(a) and (b).

As shown in the previous works, the closing of the bandgaps of TiO-terminated $LaAlO_3$ and $LaGaO_3$ results from the shift of valence band to higher energy toward the surface induced by the internal field. If the internal field is high enough, the valence band of electrons will be transferred to the lower conduction band, mainly Ti dominated density

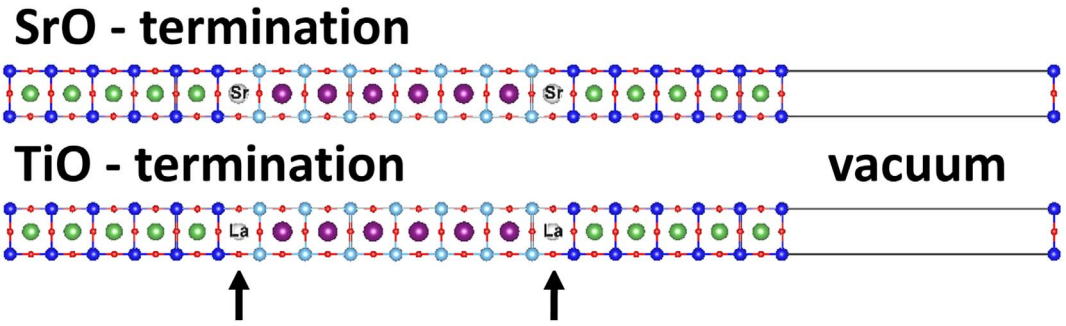

Fig. 1. Schematic structure of $ABO_3/SrTiO_3$ (001) for the density functional theory calculations. The structures consist of 6 units of $SrTiO_3$ and 6 units of ABO_3 on both sides to reduce the dipole field induced by asymmetric surfaces. The interface atoms indicated by the arrows are La for TiO-termination and Sr for SrO-termination, respectively. Here, we used 6 layers of ABO_3, where two-dimensional conducting properties in $LaAlO_3$ systems is observed.